ELSEVIER

Pyrolysis kinetics of chitin by non-isothermal thermogravimetry

Pawel Stolarek, Stanislaw Ledakowicz*

Faculty of Process and Environmental Engineering, Lodz Technical University, Wolczanska 213, 93005 Lodz, Poland

Abstract

The TGA studies of a pyrolytic decomposition of chitin obtained from arctic krill were carried out. The investigation was made at the temperature ranging from 30 to 1000 °C (303–1273 K) in the argon atmosphere at four heating rates $\beta = 2.5$, 5, 10 and 20 K min^{-1}. Two methods were used for the determination of kinetic reaction parameters: the first one involving linear regression (Kissinger's method) and the other one with the use of nonlinear regression. On the basis of isoconversion analysis of DTG curves, and literature data concerning the materials of a structure similar to chitin, four reaction groups were specified in the tested range of temperatures. A comparison of TG and DTG curves, both experimental and generated on the basis of parameters obtained, was used as a test for the correctness of calculations. Kinetic parameters obtained by the Kissinger method described process kinetics insufficiently and they were used as the starting values in the parameter estimation by the nonlinear regression method. The calculations were made for the scheme of four independent parallel reactions and four consecutive nth order reactions. Kinetic parameters E, k_0 and n obtained in this way provided a correct representation of the process kinetics although for the last group of reactions the high reaction orders ($n = 4$–5) were obtained for the two schemes of reactions. To this group at above 380 °C corresponds a mild mass loss on the TG curve. It was hypothesized, and confirmed by numerical simulation calculations, that in the region described by a high order of reaction, many reactions of first order with slightly different activation energies can take place.
© 2005 Elsevier B.V. All rights reserved.

Keywords: Biomass; Chitin; Pyrolysis; nth order kinetics

1. Introduction

Beside cellulose, chitin is the second most popular polysaccharide [1]. It is estimated that annually 10^{11} t of this biopolymer is synthesized [2]. Cellulose is synthesized mainly in plants and constitutes about 40% carbon they contain [3]. Chitin occurs primarily in the scuta of invertebrates, and also in cell walls of bacteria and mould (e.g. *Aspergillus niger*) [4]. Chitin is structurally similar to cellulose, however it is an amino polysaccharide having acetamide groups at C-2 positions in place of hydroxyl groups (Fig. 1). It forms a linear biopolymer with highly crystalline microfibrils. It is characterized by a higher degree of polymerization than cellulose [5]. Chitin is expected to have higher potential utility than cellulose in many fields [2], however chitin and cellulose

are the most important biomass resources. Chitin, as a pure biopolymer, is used mainly as a resource of carbohydrates in fodder additives. In practical applications better known is chitosan which is an acetal-free form of chitin with different deacetylation degrees, while chitin is an initial substrate for its production. Unique properties of chitin and chitosan make these biopolymers applicable in medicine and textile industry [6].

In literature there is no information on kinetic parameters of chitin pyrolysis. Knowledge of the kinetics of pyrolytic decomposition of this biopolymer can be helpful in the quantitative analysis of phenomena that occur during thermal decomposition of biological substances that may contain bacterial or fungal cells, e.g. sewage sludge. So far, the pyrolytic decomposition of chitin has been studied primarily in view of the analysis of the products of its decomposition and on this basis conclusions were drawn on its structure and mechanism of transformation [7,8]. Kinetic parameters of the pyrolysis

---
* Corresponding author. Tel.: +48 42 6313738; fax: +48 42 6313738.
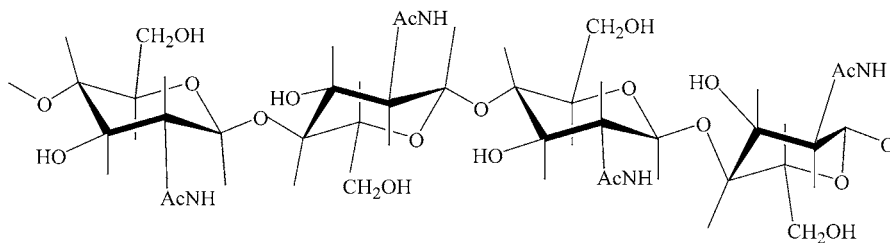 *E-mail address:* stanleda@p.lodz.pl (S. Ledakowicz).

Fig. 1. Structural scheme of chitin.

of chitosan and modified chitosan compounds are given in [9].

The goal of this study was to assess kinetic models of chitin pyrolysis and to estimate kinetic parameters of this process by means of thermogravimetry.

2. Experimental

2.1. Material

The experimental material was chitin obtained from arctic krill scuta (*Euphasia superba*) in the Sea Fishery Institute in Gdynia, Poland. The main stages of chitin production are as follows [10]:

- deproteination—accomplished most often by means of diluted soda lye whose aim was to remove both tissue proteins and those present in the form of a complex with chitin,
- demineralization—carried out most often with the use of diluted hydrochloric acid which was to decompose calcium carbonate, a mineral component of the scuta.

The next stages covered cleaning, drying and grinding of chitin.

2.2. Measuring methods

The thermogravimetric investigations were carried out on a Mettler-Toledo thermobalance model TGA/SDTA851LF. The calibration procedure was carried out according to Operating Instructions STAR^e Software. The measuring accuracy of sample temperature was checked by the onset fusion temperatures of indium ($156.6 \pm 1\,°C$) and aluminum ($660.3 \pm 1.5\,°C$) with heating/cooling dynamic segments. Kinetic parameters of the reaction should be determined with the use of thermal analysis techniques, according to the recommendations following from the ICTA research project [11–15], in non-isothermal conditions at several heating rates of sample. In this work, thermogravimetric study was carried out at the temperature ranging from 30 to $1000\,°C$ ($303–1273$ K), in dynamic conditions, at four heating rates $\beta = 2.5, 5, 10, 20$ K min^{-1} in the argon atmosphere. After reaching the temperature $1000\,°C$, pyrolytic coke was burnt in air. The sample was placed in $150\,\mu$l alumina crucible. The mass of sample was around 20 mg.

2.3. Results of measurements

Fig. 2 shows examples of experimental TG and DTG curves for the heating rate $\beta = 10$ K min^{-1}.

2.4. Kinetic models and mathematical treatment of experimental data

Determination of kinetic parameters in Eq. (1) involves the so-called kinetic triplet: activation energy E, pre-exponential factor k_0 and function of conversion $f(\alpha)$:

$$\frac{d\alpha}{d\tau} = k_0 \exp\left(-\frac{E}{RT(\tau)}\right) f(\alpha) \tag{1}$$

where α is the conversion degree in the thermogravimetric studies defined as $\alpha = (m_0 - m_\tau)/(m_0 - m_\infty)$ and $f(\alpha)$ the function that describes the reaction model.

Of vital importance is the selection of a model describing the mechanism of reaction because the values of kinetic parameters E and k_0 depend on the assumed form of function $f(\alpha)$. In the case of simple decomposition processes, procedures aiming at the model determination are used [16–18]. If, however, there are many complex reactions, this may appear impossible. The case is similar when conclusions are based on a large number of gas products obtained during the pyrolysis of chitin and other natural biopolymers [8]. So, the process is simplified by grouping the reactions that take place in a certain temperature range into the so-called lumps [19–21]. In these cases it is practically impossible to define
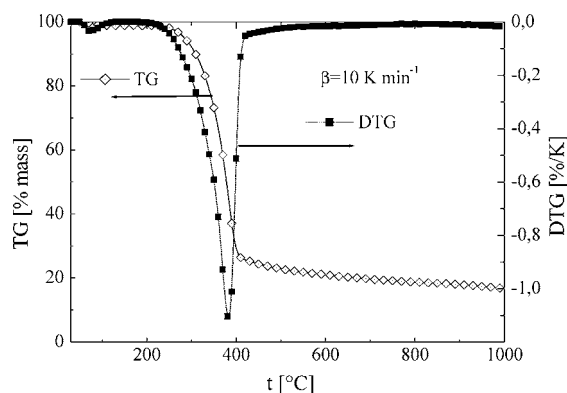
Fig. 2. TG and DTG curves for chitin at the heating rate $\beta = 10$ K min^{-1}.

a real form of the function $f(\alpha)$ therefore, the most reasonable compromise leading to a quantitative description of the process seems to be the application of the nth order reaction model for subsequent groups of reactions. A separate problem is to assume a proper reaction scheme. For this purpose, the knowledge of the mechanism of decomposition of a tested substance or any other substance with a similar structure, as well as isoconversion analysis [22] can be helpful.

There are many methods for determination of the kinetic reaction parameters on the basis of data obtained by thermal analysis methods [23–25]. The most frequently applied method for determination of the kinetic parameters is nonlinear regression [26,27]. When many parameters are sought, very important are the values of initial parameters [28,29]. An additional problem is the so-called compensation effect [30–32] which reflects interrelations between E and k_0 at a given temperature. Hence, two methods were used to find the kinetic parameters. The first one proposed by Kissinger [33] was used in a standard ASTM E 698 procedure [34]. This method is classified as a single-point method based on characteristic points of the DTG curve in the case of thermogravimetric measurements. The first test to verify correctness of the parameters obtained is to reconstruct on their basis the TG curve or a more sensitive DTG curve.

If the parameters obtained by Kissinger's method reproduced kinetic curves (TG or DTG) in an insufficient way, they would be estimated by the nonlinear regression method using the previously obtained parameters as initiating ones. Contrary to Kissinger's method that applied one point on the DTG curve, the nonlinear regression method makes use of all points on the TG or DTG curve. This two-stage methodology for the determination of parameters was used in [35–37], among the others.

2.4.1. Kissinger's method—linear regression

Kissinger's method used as a standard procedure (ASTM E698) in many computer programs applied in thermal analysis, may be difficult to employ in the case of several reactions that take place in the same temperature range (overlapping reactions). Problems related to this phenomenon were discussed elsewhere [38–40]. In order to use this method, first deconvolution of the DTG curve should be carried out onto the runs corresponding to subsequent reactions or group of reactions in the case of the lump model. Hence, the first stage was the deconvolution of the DTG curve and specification of the position of $T_{\max}$ for particular reaction group which provided a basis for determining E_i and k_{0i} from the Kissinger equation:

$$\ln\left(\frac{\beta_j}{T_{\max\ i}^2}\right) = \ln\left(\frac{Rk_{0i}}{E_i}\right) - \frac{E_i}{RT_{\max\ i}} \qquad (2)$$

First, the process complexity could be estimated on the basis of the DTG curve analysis. To assess whether one, or maybe several reactions take place, it is useful to apply the analyses proposed by Friedman [41] and Flynn–Ozawa–Wall
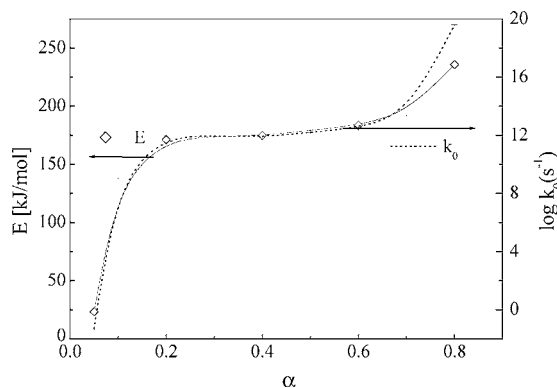

Fig. 3. Friedman's isoconversion analysis of chitin pyrolysis.

[42] by testing the variability of activation energy and pre-exponential factor during the process. Friedman's analysis is based on the form of the differential kinetic curve (DTG) (Eq. (3)) for determination of the activation energy E:

$$\ln\left[\beta_i\left(\frac{\mathrm{d}\alpha}{\mathrm{d}T}\right)_{\alpha,i}\right] = \ln(k_0)_\alpha + \ln[f(\alpha)]_i - \frac{E_\alpha}{RT_{\alpha,i}} \qquad (3)$$

and upon transformation, for determination of k_0:

$$\ln(k_0)_\alpha = \ln\left[\beta_i\left(\frac{\mathrm{d}\alpha}{\mathrm{d}T}\right)_{\alpha,i}\right] + \frac{E_\alpha}{RT_{\alpha,i}} + \ln(1 - \alpha_i) \qquad (4)$$

Flynn–Ozawa–Wall's analysis is based on the integral form of the kinetic curve (TG). The activation energy was calculated using Eq. (5):

$$\ln \beta_i = \left[\ln\left(\frac{k_0 E_\alpha}{R}\right)_{\alpha,i} - \ln[g(\alpha)]_i - 5.3305\right] - 1.052\frac{E_\alpha}{RT_{\alpha,i}} \qquad (5)$$

and upon transformation of Eq. (5), the pre-exponential factor for a given conversion degree was calculated from Eq. (6):

$$\ln(k_0)_\alpha = \ln[g(\alpha)]_i - \ln\left(\frac{E_\alpha}{R}\right) + \ln(\beta_i)$$

$$+ 5.3305 + 1.052\frac{E_\alpha}{RT_{\alpha,i}} \qquad (6)$$

Figs. 3 and 4 illustrate results of such analyses.

Two peaks can be observed on the DTG curve. The first one, as expected, is related to the dehydration process. This was confirmed by MS analyses [43]. Significant asymmetry of the other peak can suggest overlapping of several reaction groups. The isoconversion analyses indicate (Figs. 3 and 4) variations in E and k_0 with an increase of the conversion degree. This provides an evidence that the process takes place on many levels. From the shape of changes one may deduce [44] whether the process proceeds according to the scheme of concurrent or consecutive reactions. The diagram of
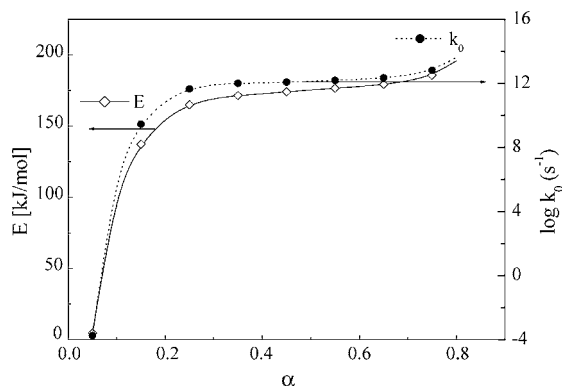
Fig. 4. Flynn–Ozawa–Wall's isoconversion analysis of chitin pyrolysis.

variability of $E = f(\alpha)$ and $k_0 = f(\alpha)$ can be divided into the three ranges:

I. the range of fast activation energy growth for $\alpha < 0.2$,
II. the range of mild activation energy growth for $0.2 < \alpha < 0.7$,
III. the range of increasing activation energy for $\alpha > 0.7$.

Low activation energies usually correspond to diffusion-controlled processes [26], in this case the dehydration at low conversion degrees. A slight increase of the activation energy in the range of α from 0.2 to 0.7 may be due to the overlapping of several reaction groups over this range, however strongly dominated by one of these groups. A further increase of the activation energy for $\alpha > 0.7$ is related to the group of reactions occurring at above 400 °C. Result of these reactions can be seen on the TG curve. It is characterized by a mild, however constant mass loss. As indicated by literature data concerning the kinetics of pyrolysis of cellulose or materials that contain cellulose, beside dehydration and volatilization at lower temperatures (up to 180 °C), three groups of reactions can be distinguished [45,46].

Assuming that the pyrolysis of chitin, a material with structure similar to that of cellulose, can proceed like that of cellulose, the DTG curve was deconvoluted (Fig. 5) into
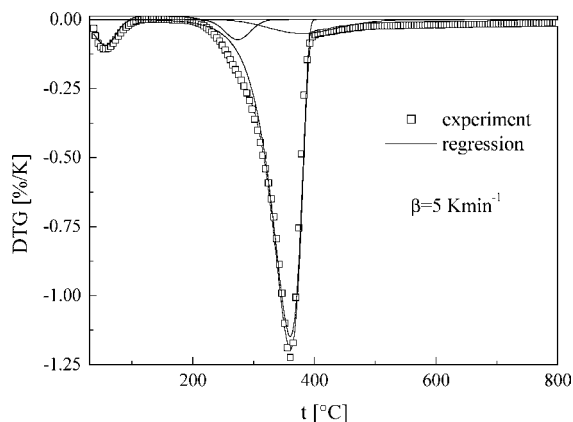
Table 1
Localization of T_{max} and areas below peaks for four lumps

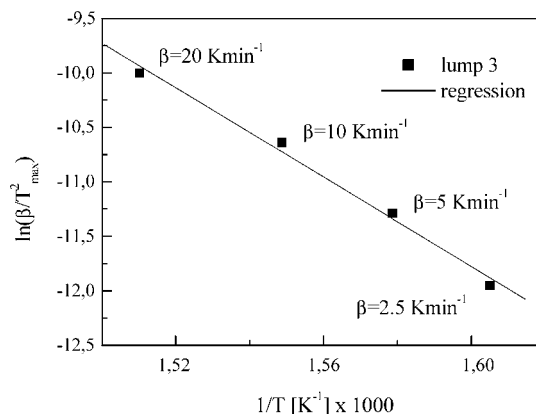| β (°C min^{-1})	Lump 1	Lump 2	Lump 3	Lump 4
Position of T_{max} (°C)				
2.5	50.7	259.1	349.9	374.5
5	56.5	273.8	360.3	379.5
10	67.9	292.8	372.6	384.2
20	75.0	313.0	389.9	387.0
Areas below peaks (%)				
2.5	5.5	2.9	81.9	9.8
5	4.5	4.2	83.4	7.9
10	1.3	5.1	82.7	10.9
20	4.9	5.0	75.3	14.7
Average	4.1	4.3	80.8	10.8

Fig. 6. Diagram for determination of the activation energy E and pre-exponential factor k_0 for lump 3.

four peaks related to particular groups of reactions:

I. Lump 1—in the temperature range 30–150 °C.
II. Lump 2—in the temperature range 150–350 °C.
III. Lump 3—in the temperature range 200–400 °C.
IV. Lump 4—in the temperature range above 350 °C.

For each lump the position of T_{max} was specified for four sample heating rates and surfaces below the peaks corresponding to the fractions of particular lumps.

Having the position of T_{max} the values of activation energy E and pre-exponential factor k_0 were determined from Eq. (2) by the linear regression. A diagram obtained on the basis of data from Table 1 for the third lump is presented (Fig. 6). The obtained values of activation energy and pre-exponential factor are given in Table 2.

On the basis of these values the TG and DTG curves were reconstructed using a scheme of four independent first-order reactions (Fig. 7).

Fig. 5. Deconvolution of the DTG curve into four lumps.

Table 2
The activation energy and pre-exponential factor estimated by Kissinger's method (ASTM E698)

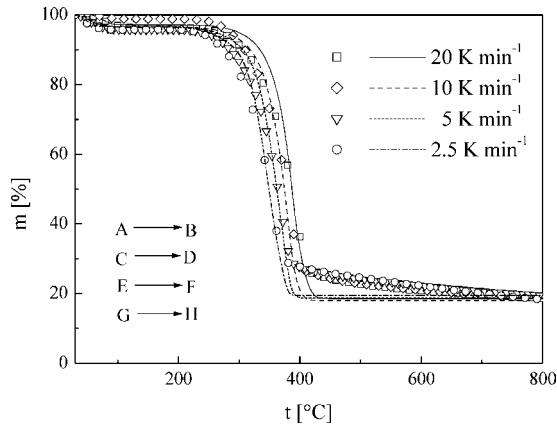|	Lump 1	Lump 2	Lump 3	Lump 4
E (kJ/mol)	69.4 ± 5.5	91.7 ± 3.2	155.3 ± 7.3	562.1 ± 51.2
$\log k_0$ (s^{-1})	8.8 ± 0.9	6.2 ± 0.3	10.4 ± 0.6	43.1 ± 4.1

Fig. 7. Comparison of experimental data with the TG curves generated by means of kinetic parameters from Table 2 (ASTM E698 method).

As shown in the diagram, parameters obtained by this method describe insufficiently the TG curve, particularly at the temperature above 400 °C. An underlying reason is the concept of Eq. (2) derived for the first-order reaction. Although Kissinger's law has been proved to be used in the models different than first-order ones [46,47], the TG curves should be reconstructed knowing such a model [48]. Actually, in the case of reaction groups, the first-order reactions could hardly be expected. Another question is high sensitivity of this method to incidental measuring errors, and problems related to deconvolution of the overlapping reactions [40].

2.4.2. Nonlinear regression

Contrary to the Kissinger's method, in which only characteristic points on DTG curves (T_{max}) are used, the nonlinear regression methods utilize all experimental points (TG or DTG curves). Optimization methods were used to find a minimum of the target function described in the case of thermogravimetric measurements (TG curve) by the equation:

$$\text{LSQ} = \sum_{j=1}^{S} \sum_{k=1}^{n} (m\exp_{j,k} - m\,\text{cal}_{j,k})^2 \tag{7}$$

or for the differential form (DTG curve)

$$\min \text{LSQ} = \sum_{j=1}^{S} f_j \sum_{k=1}^{n} \left(\frac{\text{d}m\exp_{j,k}}{\text{d}\tau} - \frac{\text{d}m\,\text{cal}_{j,k}}{\text{d}\tau} \right)^2 \tag{8}$$

where f_j is the weight coefficient standardizing all scans

$$f_j = \frac{1}{\max_k \left(\frac{\text{d}m\exp_{j,k}}{\text{d}\tau} \right)^2} \tag{9}$$

where S is the number of temperature scans; j the scan index; k the measuring point index; n the number of measuring points in a scan; $m\exp_{j,k}$ the experimental value for scan j in point k;
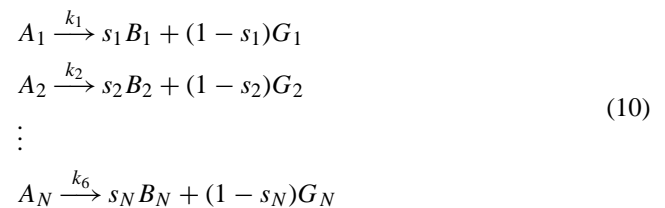
$m\,\text{cal}_{j,k}$ the calculated value for scan j in point k and $m\,\text{cal}_{j,k}$ is the solution of a system of differential equations relevant for a given reaction scheme.

In the interpretation of kinetic curves obtained from TG measurements, the mathematical models based on two reaction schemes were used:

- a scheme of four independent parallel reactions,
- a scheme of four consecutive reactions.

It is worth noting that these reaction schemes can deviate from the real, frequently unknown mechanism of pyrolysis. If, however, kinetic parameters obtained in this way provide a satisfactory quantitative description of the process and if the process rate is controlled by the chemical reaction kinetics, the results can be used for scaling up.

Provided the tested sample consists of N chemical substances that are degraded in the measurement conditions, the reaction scheme assumes the following form:
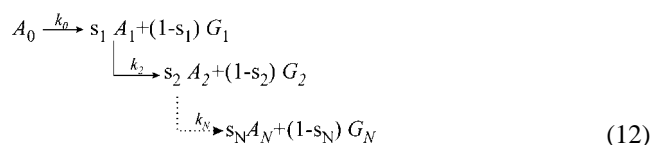
$$A_1 \xrightarrow{k_1} s_1 B_1 + (1 - s_1)G_1$$
$$A_2 \xrightarrow{k_2} s_2 B_2 + (1 - s_2)G_2$$
$$\vdots \tag{10}$$
$$A_N \xrightarrow{k_6} s_N B_N + (1 - s_N)G_N$$

where A_i denotes a substrate that takes part in the ith reaction, B_i the stable solid product of this reaction, and G_i is the gas product, while the stoichiometric coefficient s_i denotes the ratio of solid product mass to the mass of reacted substrate.

The kinetic model corresponding to the parallel reactions scheme can be written by the following system of ordinary differential equations:

$$\frac{\text{d}a_1}{\text{d}\tau} = k_{01} \exp\left(-\frac{E_1}{RT(\tau)} \right) f_1(a_1), \quad a_1(0) = 1$$
$$\vdots \tag{11}$$
$$\frac{\text{d}a_N}{\text{d}\tau} = k_{0N} \exp\left(-\frac{E_N}{RT(\tau)} \right) f_N(a_N), \quad a_N(0) = 1$$

where $a_i = m_{A_i}/m_{0A_i}$; m_{A_i} the substrate mass A_i; m_{0A_i} the initial substrate mass A_i and $f(a_i)$ is the form of the function describing the reaction model—the functions corresponding to the first and nth order reactions were taken for calculations.

If sample decomposition proceeded according to the consecutive reaction scheme, then:

$$A_0 \xrightarrow{k_0} s_1\,A_1 + (1\text{-}s_1)\,G_1$$
$$\qquad \xrightarrow{k_2} s_2\,A_2 + (1\text{-}s_2)\,G_2$$
$$\qquad \vdots \xrightarrow{k_N} s_N A_N + (1\text{-}s_N)\,G_N \tag{12}$$

while the kinetic model was described by the following system of differential equations:

$$\frac{da_0}{d\tau} = k_{01} \exp\left(-\frac{E_1}{RT(\tau)}\right) f_1(a_0), \quad a_0(0) = 1$$

$$\frac{da_1}{d\tau} = k_{01} \exp\left(-\frac{E_1}{RT(\tau)}\right) f_1(a_0)$$

$$- k_{02} \exp\left(-\frac{E_2}{RT(\tau)}\right) f_2(a_1), \quad a_1(0) = 0$$

$$\vdots \qquad\qquad (13)$$

$$\frac{da_{N-1}}{d\tau} = k_{0N-2} \exp\left(-\frac{E_{N-2}}{RT(\tau)}\right) f_{N-2}(a_{N-2})$$

$$- k_{0N-1} \exp\left(-\frac{E_{N-1}}{RT(\tau)}\right) f_{N=1}(a_{N-1}),$$

$$a_{N-1}(0) = 0$$

and

$$a_N = 1 - \sum_{i=0}^{N-1} a_i$$

Solution of the equation system in the kinetic model of reaction makes it possible to calculate the values of $m\,cal$ in Eq. (7) from the following relation:

$$m\,cal = m_0 - \alpha \Delta m$$

where

$$\alpha = \sum_{i=1}^{N} w_i(1 - a_i) \quad \text{for parallel reactions}$$

$$\alpha = \sum_{i=1}^{N} \left(w_i \sum_{j=i}^{N} a_j\right) \quad \text{for consecutive reactions}$$

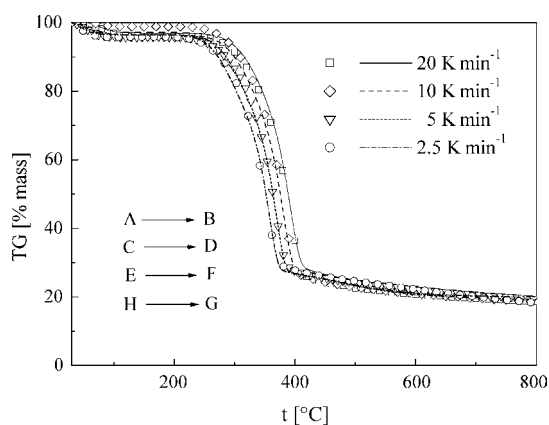$$w_i = \frac{\Delta m_i}{\Delta m}, \quad i = 1, 2, \ldots, N$$

Table 3
Kinetic parameters of chitin pyrolysis models estimated by the nonlinear regression method

	Reaction scheme	
	Consecutive reactions	Parallel reactions
Kinetic parameters		
$\log k_{01}$ (s^{-1})	7.3	7.1
E_1 (kJ/mol)	60.8	59.2
n_1	1.3	1.5
$\log k_{02}$ (s^{-1})	10.9	8.4
E_2 (kJ/mol)	145.6	121.8
n_2	0.9	2.4
$\log k_{03}$ (s^{-1})[1]	10.41	13.57
E_3 (kJ/mol)	153.1	195.7
n_3	1.1	0.7
$\log k_{04}$ (s^{-1})	3.7	9.8
E_4 (kJ/mol)	69.7	182.5
n_4	4.0	5.0
Fraction of reaction 1	4.1E−02	4.4E−02
Fraction of reaction 2	0.1	0.4
Fraction of reaction 3	0.6	0.5
Statistics for TG curve		
Sum of square deviations	6540.77543	2566.77555
Mean square error	2.83991	1.77903
Correlation coefficient	0.998603	0.999398
Statistics for DTG curve		
Sum of square deviations	0.14248	2.591E−02
Mean square error	1.324E−02	5.652E−03
Correlation coefficient	0.976838	0.996364

where Δm denotes the total mass loss reported in the experiment.

The minimum of function (7) was searched by the nonlinear regression method using Levenberg–Marquardt optimization procedure. The optimizing parameters were constants in the Arrhenius equation, reaction orders (for the nth order reaction) and the fraction of w_i of the reactions in the total mass loss. The system of differential mass balance equations was integrated by fifth-order Runge–Kutta method or Rosenbrock's method. The initiating parameters resulted from the previous estimations of Kissinger's method. Table 3 gives
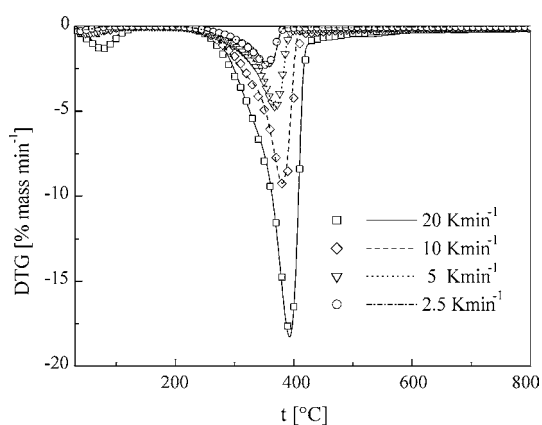

Fig. 8. TG curve of chitin pyrolysis. Approximation of experimental results by four parallel nth order reactions.

Fig. 9. DTG curve of chitin pyrolysis. Approximation of experimental results by four parallel nth order reactions.
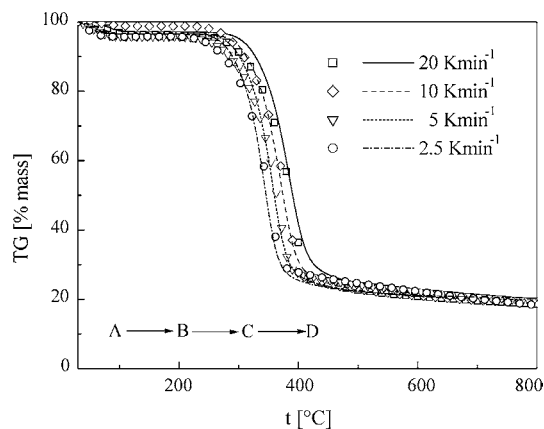
Fig. 10. Comparison of experimental and calculated TG curves for four consecutive *n*th order reactions (kinetic parameters obtained by nonlinear regression).
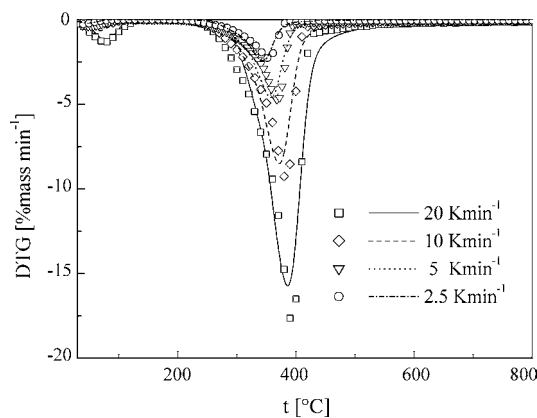

Fig. 11. Comparison of experimental and generated DTG curves for four consecutive *n*th order reactions (kinetic parameters obtained by nonlinear regression).

kinetic parameters obtained by the nonlinear regression method for four independent parallel and consecutive reactions, respectively.

Figs. 8–11 show the TG and DTG curves reconstructed on the basis of data given in Table 3 for the scheme of four concurrent and four consecutive reactions, respectively.

The kinetic parameters obtained from nonlinear regression reconstruct TG and DTG curves in a satisfactory way. Slightly better fitting was obtained for parallel reactions, however, the consecutive reaction scheme is closer to the real mechanism of biopolymer decomposition.

3. Comments and discussion

When analyzing TG and DTG curves and comparing them to results presented in the literature for cellulose or hemi-cellulose, it is worth noting that the maximum rate of chitin decomposition is shifted towards higher temperatures. In parallel, the DTG diagram is characterized by a very steep and narrow peak which indicates a fast sample decomposition in a narrow range of temperatures. Font [49] states that the maximum decomposition rate for the heating rate $\beta = 10\,\mathrm{K\,min^{-1}}$ for hemicellulose is at around 310 °C, for cellulose at about 368 °C, while for chitin the maximum decomposition rate observed in this study ranges from 350 to 380 °C depending on the heating rate. The decomposition temperature is related to the degree of biopolymer polymerization [8,50] and for chitin DP is about 2000–5000 [2]. As reported by Moldoveanu [8], during chitin pyrolysis secondary condensation reactions occur that result in the formation of three-dimensional polymer structures containing −N−C−C−N− bonds which are decomposed only at higher temperatures. All these factors cause that temperature ranges in which thermal decomposition of these substances takes place, are different. At the same time, high energy supplied along with higher temperature causes that once initiated reactions of decomposition take place vehemently. This can be due to a free-radical character of these reactions.

To estimate the kinetic parameters, the scheme of independent parallel and consecutive reactions was applied. It is doubtful in the case of pure biopolymers that the scheme of concurrent reactions reflects the mechanism of transformations, however, such a simplified scheme is often assumed to estimate the kinetic parameters of biopolymers [20,51]. As reported in the literature, the values of kinetic parameters depend on the selection of function $f(\alpha)$ related to the model of reaction and the scheme of reactions [48]. Low values of activation energy reaching ca. 60 kJ/mol, obtained for the first group of reactions (dehydration, volatilization) indicate that the process has a diffusive character [26]. The orders of reaction at this stage range from 1.3 to 1.5.

Most troublesome in the estimation of kinetic parameters appeared to be the last group of reactions describing the process at above 400 °C, when after a period of quick mass changes, an almost linear and slow process was observed, and on the DTG curve is almost invisible and negligible. In that case the rate of mass loss was almost constant. However, this stage is manifested on the TG curve and cannot be neglected. Such shape of the TG and DTG curves was obtained also by other researchers for the pyrolysis of pure biopolymers [45,52–55]. In this case it might be difficult to estimate the kinetic parameters on the basis of DTG data, although the DTG curve is more sensitive than the TG curve and is a better test for assessing if the obtained kinetic parameters are correct. The kinetic parameters obtained from the DTG curve did not provide a good mapping of the TG curve and vice versa. When high orders of the reaction were accepted, fitting of the model to experimental results was much better.

Hardly acceptable orders of reaction can be found in literature e.g. Conesa et al. [56] proposed for example $n = 23$. The same value of reaction order for the decomposition of residual of cellulose pyrolysis was estimated by Capart et al. [52] with the use of the nucleation-growth model. This can be taken as one of the mathematical parameters which facilitate the process description. The authors [52] explained that
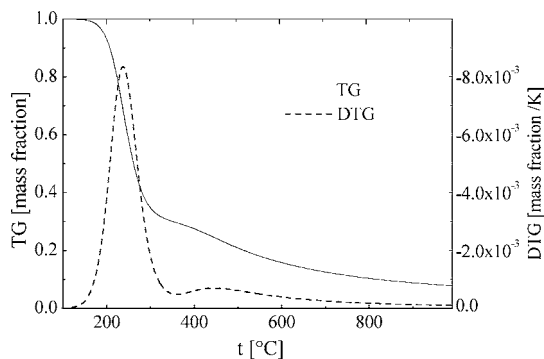
Fig. 12. The TG and DTG curves generated for two parallel reactions.

Fig. 13. TG and DTG curves generated for seven parallel reactions.

reaction order $n > 2$ is mathematically equivalent to Gamma distribution of frequency factors. The interpretation of high values of reaction order has been discussed in the literature e.g. a good overview is given by Burnham and Braun [57]. However, the reason why this parameter has such a high value in relation to the described phenomena has not been completely explained.

This work tries to provide an explanation. At the first stage it was checked if actually a high order of the reaction could give a mild mass loss on the TG curve. For this purpose the TG and DTG curves were generated for the model of two independent parallel reactions of the same values of E and k_0. The only difference was the share and order of the reaction. The following parameters were assumed in the simulation:

Reaction 1 : $E_1 = 100\,\text{kJ/mol};\quad k_{01} = 10^{10}\,\text{min}^{-1};$
$$m_{01} = 0.7;\quad n_1 = 2$$

Reaction 2 : $E_2 = 100\,\text{kJ/mol};\quad k_{02} = 10^{10}\,\text{min}^{-1};$
$$m_{02} = 0.3;\quad n_2 = 8$$

Fig. 12 shows the TG and DTG curves generated on the basis of these data for the heating rate $\beta = 10\,^\circ\text{C min}^{-1}$.

As shown in Fig. 12, the shape of TG and DTG curves is close to the one obtained for experimental data for chitin (Fig. 2). The TG curve consists of a steep segment (the first reaction is predominant in the temperature range 200–300 °C) and the second segment with mild mass loss for the second reaction above 300 °C. The latter segment on the DTG curve is characterized by a small and almost constant rate of mass loss. Hence, high order of reaction in this case (note that here $n = 8$) cannot arouse doubts, at least from the mathematical point of view. How can we then explain these high orders in the process description when, at least theoretically, the order of reaction should not exceed 2?

As it has been mentioned, when the lump model is applied in the process description, the reactions are grouped according to their appearance in particular temperature ranges. It was hypothesized that in the higher temperature range the kinetics of the lumped reactions described by a high reaction order could be replaced by many reactions of first order with
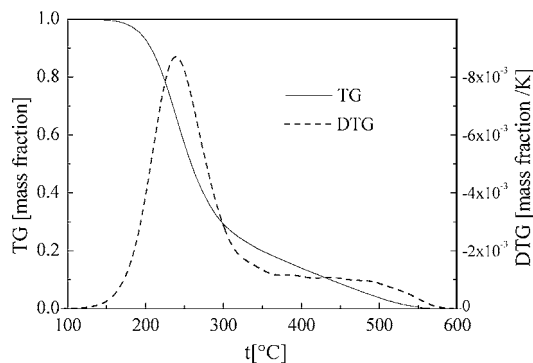
slightly different values of the activation energy. To verify this, one should generate such TG curve that would yield a linear or close to linear mass loss in the conditions of dynamic heating of the sample. Such relation was generated for seven parallel reactions for the following kinetic parameters:

Reaction 1 : $E_1 = 100\,\text{kJ/mol};\quad k_{01} = 10^{10}\,\text{min}^{-1};$
$$n_1 = 2;\quad m_{01} = 0.7$$

Reactions 2–7 : E_2–E_7 changing linearly from

110 kJ/mol by step, $\quad \Delta E = 10\,\text{kJ/mol};$

$k_{02} = k_{03} = \cdots = k_{07} = 10^{10}\,min^{-1};$

$n_2 = n_3 = \cdots = n_7 = 1;$

$m_{02} = m_{03} = \cdots = m_{07} = 0.05$

Fig. 13 illustrates the TG and DTG curves generated for these assumed kinetic parameters. The curve shape reveals characteristic features observable during decomposition of many bipolymers or biological materials, and the region of mild, nearly linear mass loss, gives in such cases high orders of reaction when the kinetic parameters are estimated by means of nonlinear regression. Comparing the TG and DTG generated curves (Fig. 13) with experimentally obtained ones for chitin pyrolysis (Fig. 2) we can conclude that they are very similar. It could be possible to better fit the experimental data by manipulation of partial mass losses m_i corresponding to individual reactions in the region of higher temperature.

4. Conclusions

Summarizing the experimental results and discussion on chitin pyrolysis one can conclude:

- a maximum rate of chitin decomposition was observed in a higher temperature range (350–380 °C) than in the case of biopolymers described in literature that had a similar structure like cellulose, and as might be expected, this is related to a higher degree of polymerization in the case of chitin,

- when the reaction mechanism of pyrolysis is unknown, the Kissinger's method can prove to be unreliable and the first test for verifying correctness of the results obtained, can be a comparison of experimental TG curves and those generated on the basis of kinetic parameters, in particular the comparison of more sensitive DTG curves is advisable,
- in the tested temperature range of pyrolysis the four reaction groups were found, and kinetic parameters obtained by means of nonlinear regression, described correctly the quantitative pyrolytic decomposition of chitin both for independent parallel and consecutive reaction schemes,
- high reaction orders obtained for the chitin decomposition above 400 °C were interpreted as a group of many reactions of first reaction order with slightly increasing activation energies, however above 100 kJ/mol.
- slightly better fitting was obtained for four parallel reactions, however, the consecutive reaction scheme seems to be more physically plausible mechanism as the calculated values of reaction orders are closer to unity.

References

[1] H.G. Schlegel, Allgemeine Mikrobiologie, G. Thieme Verlag, Stuttgart, 1976.
[2] K. Kurita, Prog. Polym. Sci. 26 (2001) 1921.
[3] C. Saint-Jimenez, Naturwissenschaften 81 (1994) 451.
[4] M.N.V. Ravi Kumar, Reactive Func. Polym. 46 (2000) 1.
[5] H. Struszczyk, Progress on Chemistry and Application of Chitin and its Derivatives, vol. VI, Monograph of the Polish Chitin Society, 2000, p. 79.
[6] D. Van Luyen, V. Rossbach, Techn. Textillien, März (1992) 35.
[7] R. Marbot, J. Appl. Pyrolysis 39 (1997) 97.
[8] S.C. Moldoveanu, Analytical Pyrolysis of Natural Organic Polymers, Techniques and Instrumentation in Analytical Chemistry, vol. 20, Elsevier, Amsterdam, 1998.
[9] A. Pawlak, M. Mucha, Thermochim. Acta 396 (2003) 153.
[10] M. Brzeski, M. Mieczkowska, K. Sowa, H. Stolz, A. Wojcieszak-Pająk, W. Neugebauer, Chityna, Chitozan. Produkcja i wykorzystanie, Seria S, No. 2, 13, Morski Instytut Rybacki, Gdynia-Poland, 1985 (in Polish).
[11] M.E. Brown, M. Maciejewski, S. Vyazovkin, R. Nomen, J. Sempere, A.K. Burnham, J. Opfermann, R. Strey, H.L. Anderson, A. Kemmler, R. Keuleers, J. Janssens, H.O. Desseyn, Ch.R. Li, B.T. Tang, B. Roduit, J. Malek, T. Mitsuhashi, Thermochim. Acta 355 (2000) 125.
[12] M. Maciejewski, Thermochim. Acta 355 (2000) 145.
[13] S. Vyazovkin, Thermochim. Acta 355 (2000) 155.
[14] A.K. Burnham, Thermochim. Acta 355 (2000) 165.
[15] B. Roduit, Thermochim. Acta 355 (2000) 171.
[16] J. Militky, J. Sestak, Thermochim. Acta 203 (1992) 31.
[17] S. Vyazovkin, A.I. Lesnikovich, J. Therm. Anal. 35 (1989) 2169.
[18] A.K. Galwey, M.E. Brown, in: M.E. Brown (Ed.), Handbook of Thermal Analysis and Calorimetry, vol. 1: Principles and Practice, Elsevier Science B.V, 1998 (Chapter 3).
[19] A.N. Garcia, A. Marcilla, R. Font, Thermochim. Acta 254 (1995) 277.
[20] H. Teng, H.-Ch. Ling, J.-A. Ho, Ind. Eng. Chem. Res. 36 (1997) 3974.
[21] E. Ranzi, M. Dente, A. Goldaniga, G. Bozzano, T. Faravelli, Prog. Energy Comb. Sci. 27 (2001) 99.
[22] S. Vyazovkin, Int. J. Chem. Kinet. 28 (2) (1996) 95.
[23] J.H. Flynn, L.A. Wall, J. Res. Natl. Bur. Stand. A: Phys. Chem. 70A (6) (1966) 487.
[24] J.R. MacCallum, J. Tanner, Eur. Polym. J. 6 (1970) 907.
[25] J.R. MacCallum, J. Tanner, Eur. Polym. J. 6 (1970) 1033.
[26] J. Šestak, J. Therm. Anal. 16 (1979) 503.
[27] P. Ahuja, S. Kumar, P.C. Singh, Chem. Eng. Technol. 19 (1996) 272.
[28] H.L. Anderson, A. Kemmler, R. Strey, Thermochim. Acta 271 (1996) 23.
[29] V. Slovák, Thermochim. Acta 372 (2001) 175.
[30] A. Mianowski, J. Therm. Anal. 74 (2003) 95.
[31] A. Mianowski, R. Bigda, J. Therm. Anal. 74 (2003) 974.
[32] M.E. Brown, A.K. Galwey, Thermochim. Acta 387 (2002) 173.
[33] H.E. Kissinger, J. Res. Natl. Bur. Stand. 57 (1956) 217.
[34] ASTM Committee on Standards, ASTM E 698, Annual Book of ASTM Standards, 1984.
[35] R.L. Braun, A.K. Burnham, Energy and Fuel 1 (1987) 153.
[36] T. Fisher, M. Hajaligol, B. Waymack, D. Kellogg, J. Anal. Appl. Pyrol. 62 (2) (2002) 331.
[37] C.J. Gomez, J.J. Manya, E. Velo, L. Puigjaner, Ind. Eng. Chem. Res. 43 (2004) 901.
[38] F.W. Wilburn, Thermochim. Acta 340/341 (1999) 77.
[39] F.W. Wilburn, Thermochim. Acta 354 (2000) 99.
[40] P. Stolarek, S. Ledakowicz, Inzynieria Chemiczna i Procesowa 24 (2003) 701 (in Polish).
[41] H.L. Friedman, J. Appl. Polym. Sci., Part C 6 (1964) 183.
[42] J. Flynn, L.A. Wall, Polym. Lett. 4 (1966) 232.
[43] P. Stolarek, Kinetics of pyrolysis of sewage sludge and selected components of biomass, Ph.D. Thesis, Department of Bioprocess Engineering, Technical University of Lodz, Poland, 2004.
[44] S. Vyazovkin, A.I. Lesnikovich, J. Therm. Anal. 36 (1990) 599.
[45] J.J. Manya, E. Velo, L. Puigjaner, Ind. Eng. Chem. Res. 42 (2003) 434.
[46] H.E. Kissinger, Anal. Chem. 11 (29) (1957) 1702.
[47] D. Chen, X. Gao, D. Dollimore, Thermochim. Acta 215 (1993) 109.
[48] M.A. Bastow, Comput. Geosci. 21 (9) (1995) 1015.
[49] R. Font, A. Marcilla, A.N. Garcia, J.A. Caballero, J.A. Conesa, J. Anal. Appl. Pyrolysis 32 (1995) 29.
[50] P. Wandelt, Technologia celulozy i papieru. Cz 1. Technologia mas włóknistych, WSiP, Warszawa, 1996 (in Polish).
[51] G. Vàrhegyi, M.J. Antal Jr., E. Jakab, P. Szabó, J. Anal. Appl. Pyrolysis 42 (1997) 73.
[52] R. Capart, L. Khezami, A.K. Burnham, Thermochim. Acta 417 (2004) 79.
[53] Y. Wu, D. Dollimore, Thermochim. Acta 324 (1998) 49.
[54] J.A. Conesa, A. Marcilla, J.A. Caballero, R. Font, J. Anal. Appl. Pyrolysis 58/59 (2001) 617.
[55] N.E. Marcovich, M.M. Reboredo, M.I. Aranguren, Thermochim. Acta 372 (2001) 45.
[56] A. Conesa, A. Marcilla, D. Prats, Rodriguez-Pastor, Waste Manage. Res. 15 (1997) 293.
[57] A.K. Burnham, R.L. Braun, Energy and Fuel 13 (1999) 1.